

or from an excited doublet $\sim 5 \text{ cm}^{-1}$ above the ground state. As seen from Fig. 1(c), however, the absorption falls instead of rising with decreasing temperature. We conclude that this resonance is saturated and hence the resonance observed at the considerably lower temperatures used by Kirton and Newman is a fortiori saturated.

We are grateful to Dr. J. R. Shane for many helpful discussions, to Dr. R. Newman and Dr. R. Damon for their interest and suggestions, and to Mr. R. J. Brophy for performing the resonance experiments.

¹R. W. Kedzie, D. H. Lyons, and M. Kestigian, Phys. Rev. 138, A918 (1965). We wish to point out that, de-

pending on the choice of sign in Eqs. (8)-(11) of this reference, the $g=4.3$ resonance arises from either a ground (Fig. 7) or an excited (Fig. 6) doublet, without altering the basic interpretation in this reference. Thus, observation of depopulation of the resonance, if it occurred, would not decide between the theory of this reference and that of T. Castner, Jr., G. S. Newell, W. C. Holton, and C. P. Slichter, J. Chem. Phys. 32, 668 (1960), as erroneously stated in J. Kirton and R. C. Newman, Phys. Rev. Letters 15, 244 (1965).

²Kirton and Newman, reference 1.

³W. B. Mims, K. Nassau, and J. D. McGee, Phys. Rev. 123, 2059 (1961).

⁴R. W. Kedzie, J. R. Shane, and M. Kestigian, Phys. Letters 11, 286 (1964).

⁵A. M. Portis, Phys. Rev. 91, 1071 (1953).

⁶M. W. P. Strandberg, Microwave J. 4, 66 (1961).

⁷T. Castner, Jr., G. S. Newell, W. C. Holton, and C. P. Slichter, J. Chem. Phys. 32, 668 (1960).

OBSERVATIONS ON THE FERMI SURFACE OF ALUMINUM BY NEUTRON SPECTROMETRY

R. Stedman and G. Nilsson

AB Atomenergi, Studsvik, Sweden
(Received 13 September 1965)

We have determined the dispersion relations for phonons in aluminum at 80 and 300°K by slow-neutron spectrometry, using a three-axis crystal spectrometer at the 30-MW research reactor R2 in Studsvik.¹ Initial detailed measurements on a single dispersion curve failed to reveal Kohn anomalies of the kind reported by Brockhouse, Rao, and Woods² for lead, but later supplementary measurements in selected regions and an improved analysis of data have revealed such effects. They are too small to be obvious by direct inspection of a series of points on a dispersion curve, but the data are sufficiently accurate to allow the variation of slope along a curve to be followed, utilizing average values of the slope in the interval between two successive points, and to see irregularities which are significant in relation to the errors involved. This improved analysis has been applied to all data. Even on curves of slope versus wave number the effects are still not large, but we have two independent series of measurements (at 80 and 300°K) and the shapes of observed one-phonon resonances to refer to, and on this basis feel justified in assigning eight points on the Fermi surface of aluminum.

Figure 1 shows the expected sites of Kohn anomalies in aluminum. The construction is

to draw the intersections of spheres with the triangular surface indicated; each sphere is of radius $2\rho_F$ and has its center at a reciprocal lattice point. The radius ρ_F of the Fermi sphere for free electrons is 1.13 (on the same scale as the figure; this scale is used for all wave vectors here). Circles derived from lattice points outside the plane of the figure are dashed. The intersection of two circles is "rounded off" if the centers of the spheres concerned are separated by twice a lattice vector—corresponding to Bragg reflection of electrons and gap formation. The rounding-off is schematic, and does not attempt to follow theoretical descriptions of the Fermi surface. The

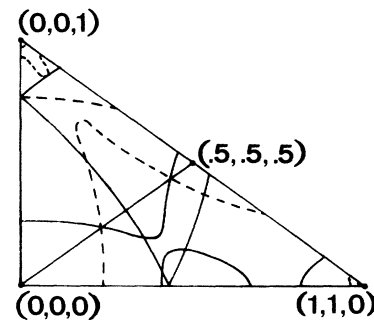


FIG. 1. Estimated positions of Kohn anomalies for a near-spherical Fermi surface.

figure is a guide to the positions and expected sizes of anomalies: The positions are indicated by the modified circular arcs, the sizes by the following line of reasoning.

If ω is the phonon frequency, ω^2 may be expressed as a sum of various terms, and the part of this sum which figures in the Kohn anomalies is³

$$\sum_{\vec{G}} (\vec{Q} \cdot \vec{\epsilon}/Q)^2 F(Q), \quad (1)$$

where \vec{G} is any reciprocal lattice vector, \vec{Q} is the wave vector of a phonon, referred to the lattice point \vec{G} , and $\vec{\epsilon}$ is the polarization vector of the phonon. For a metal such as aluminum this formula is expected to be a fair approximation, except where the departure of the Fermi surface from sphericity is pronounced, i.e., near Bragg planes. The densities of states involved in the electron transition may vary markedly in such regions: A flattening of the Fermi surface should give a larger Kohn effect, and vice versa. The anomalies arise from the behavior of $F(Q)$ when $Q = 2\rho_F$ (spherical Fermi surface), and the relative size of an anomaly in a particular material will therefore be proportional to the product of what we may call the multiplicity and the polarization factor. The multiplicity is the number of \vec{G} vectors contributing simultaneously to (1) at the anomaly concerned; the polarization factor is $(\vec{Q} \cdot \vec{\epsilon}/Q)^2$. What has just been said applies to a Kohn anomaly in the curve of ω^2 vs q . For a dispersion curve, the expected relative size of an anomaly is given by (multiplicity) \times (polarization factor)/ ω .⁴ In order that this quantity shall be dimensionless, ω should be taken relative to a given frequency; taking the latter to be 10^{13} rad/sec⁻¹, we arrive at the values given in Table I. The anomalies there are numbered from the origin in accordance with Fig. 1.

A positive sign indicates an upward anomaly, a negative sign a downward. The figures for "split" anomalies $-(2, 0, 0)$: 3 and 4; $(2, 2, 0)$: 4 and 5; $(2, 2, 0)$: 6 and 7—give poor guidance (are probably too high), except as regards the relation between the various branches. The simple reasoning used here is quite invalid at Bragg planes.

Figure 2 shows slope versus q for the $(1, 1, 1)$ L and T curves and for the $(2, 0, 0)$ L and T curves. The points at $q=0$ are from sound-velocity data.⁵ It will be seen that points for 80 and 300°K combine very well (except near the origin where those for 300°K are lower, as expected), and indicate that assigned errors are conservative. These errors arise mainly from the estimated errors for the original frequencies. Individual points with associated errors are not independent in the usual sense because possible curves through them are subject to the condition that the area under the curve is quite well defined even in an interval $\Delta q = 0.2$. Similar plots to those of Fig. 2 for the three $(2, 2, 0)$ branches are not shown, though results for them are quoted below.

In the $(1, 1, 1)$ direction all three anomalies are apparent. Anomalies 1 and 2 are close together on the L branch. From the figure and markedly distorted peaks at $q = 0.52$ and $q = 0.56$, No. 2 is at 0.52 ± 0.04 . No. 1 is weaker than expected, presumably because of proximity to Bragg planes (cf. Fig. 3); we take it to be at 0.42 ± 0.03 . No. 3 is at 0.72 ± 0.03 (cf. T branch).

In the $(2, 0, 0)$ direction anomalies 1 and 2 are apparent. No. 1 is at 0.23 ± 0.02 , No. 2 at 0.83 ± 0.03 . It seems that anomaly 3 occurs at 0.95 ± 0.03 ; this conclusion is dubious merely on the basis of Fig. 2(b), but from the observation of anomaly 6 in the $(2, 2, 0)$ direction (see below) is plausible.

In the $(2, 2, 0)$ direction, anomaly 1 cannot

Table I. Expected positions and relative sizes of Kohn anomalies in aluminum. Units: see text.

Anomaly No.	(1, 1, 1) direction			(2, 0, 0) direction			(2, 2, 0) direction			
	q	Relative size		q	Relative size		q	Relative size		
		L	T		L	T		L	T_1	T_2
1	0.41	+0.4	+0.4	0.26	+0.4	0	0.35	+0.3	0	+0.4
2	0.55	+0.2	0	0.77	+0.4	+0.2	0.57	-0.2	0	0
3	0.75	-0.2	-0.3	0.92	-0.1	-0.2	0.61	+0.3	+0.1	0
4				0.98	-0.1	-0.2	0.95	0	+0.2	0
5							1.15	0	+0.2	0
6							1.34	-0.2	-0.1	-0.2
7							1.40	-0.2	-0.1	-0.2

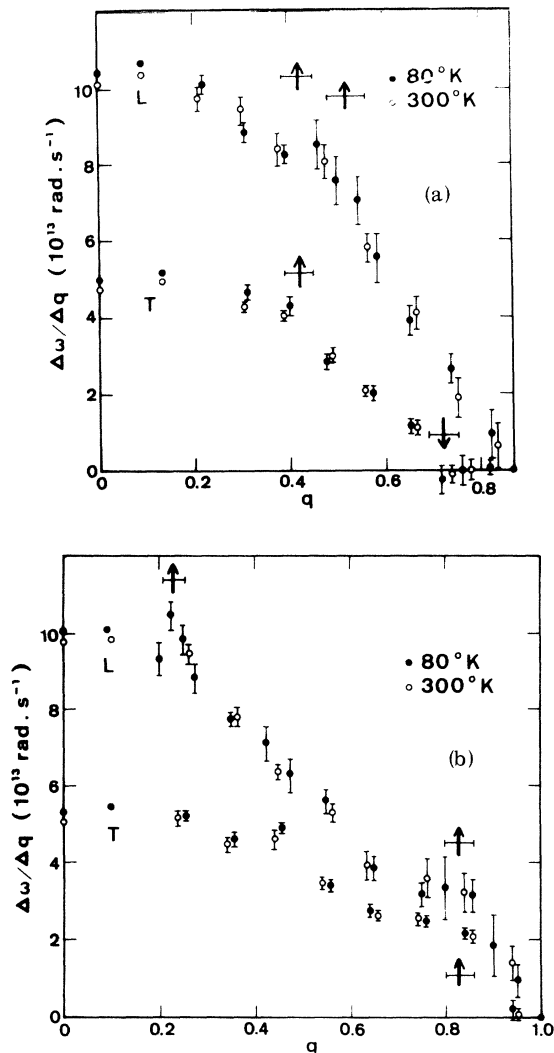


FIG. 2. Variations of slope along dispersion curves (a) in the (1, 1, 1) direction; (b) in the (2, 0, 0) direction.

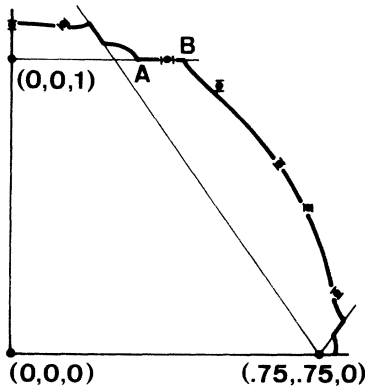


FIG. 3. Points from our results in relation to the Fermi surface as given by Segall.⁶

be seen in the L branch, and can be only roughly located on the T_2 branch because of an omission in our measurements. Anomaly 2 cannot be seen; the high curvature of the Fermi surface would probably make it weak. Anomaly 3 occurs at 0.63 ± 0.02 on the L branch, and anomaly 6 at 1.33 ± 0.03 on the T_2 branch (perhaps on the L branch as well, though the large curvature of the dispersion curve obscures the effect). A distinct upward anomaly in the T_1 branch at 1.06 ± 0.04 does not seem to correspond to either No. 4 or No. 5: It is unexpectedly large, apparently unaccompanied by its "pair," and in an unlikely position. It can be explained in terms of a nondiametral electron transition: If the points diametrically opposite to A and B in Fig. 3 are A' and B' , it will be seen that transitions near $A' - B$ and $B' - A$ are between regions of more nearly parallel shapes than the diametral transitions $A' - A$ and $B' - B$. Moreover, they reinforce one another. With this interpretation, the anomaly corresponds to a point midway between 4 and 5. If this interpretation is correct it should apply to all split anomalies.

Points on the Fermi surface corresponding to six of the above anomalies are shown in Fig. 3, which is a section through the Fermi surface given by Segall.⁶ A seventh point in the middle of the AB gap is in accordance with the explanation offered above. The other two anomalies—mentioned above as $(2, 0, 0)$: 3 and $(2, 2, 0)$: 6—are more tentative individually. They are both close to $(1, 0, 0.5)$ (W), however, and thus lend support to one another. In the light of what has been said above about split anomalies and the circumstance that three Bragg planes meet at W , it is not certain what such anomalies correspond to, but it does seem that, whatever the structure of the Fermi surface near W , the main surface comes near to W . This agrees with the conclusion that the fourth-zone pockets are empty,^{7,8} and (less definitely) that the Harrison monster is dismembered.⁷

A rough estimate of the magnitude of anomalies in aluminum (steps in dispersion curves) may be made from three of them which correspond to points on the Fermi surface far from Bragg planes (cf. Fig. 3), and for which the estimates of Table I may be reasonable. In frequency units 10^{13} rad/sec the resulting figure is (0.3 ± 0.15) times the estimated relative strength as given in Table I.

No attempt has been made to interpret an

anomaly at $q=0.45$ in the T branch of Fig. 2(b). An explanation might be obtained in terms of an extreme value of \bar{Q} associated with a markedly nonspherical region of the Fermi surface, but in the present incomplete state of our results such a special case does not seem to warrant much speculation. A similar unexplained anomaly appears to occur at $q=0.35$ in the $(2, 2, 0) T_1$ branch. To examine such effects, and to check and extend our observations, further precise measurements are desirable.

¹A preliminary report was given in the Proceedings of the International Atomic Energy Agency Symposium on the Inelastic Scattering of Neutrons, Bombay, India, 1964 (International Atomic Energy Agency, Vienna, 1965), Vol I, p.211. A full account will be published soon.

²B. N. Brockhouse, K. R. Rao, and A. D. B. Woods, *Phys. Rev. Letters* **7**, 93 (1961).

³See, for instance, S. H. Vosko, R. Taylor, and G. H. Keech, *Can. J. Phys.* **43**, 1187 (1965); also, E. J. Woll and W. Kohn, *Phys. Rev.* **126**, 1693 (1962).

⁴The occurrence of ω in the denominator here indicates, incidentally, one important reason why anomalies are easier to see in lead, where phonon frequencies are a factor five less than in aluminum. A preliminary comparison of the results for aluminum and results at present being obtained by us for lead indicates that anomalies in aluminum and lead are of comparable sizes in curves of ω^2 vs q .

⁵G. N. Kamm and G. A. Alers, *J. Appl. Phys.* **35**, 327 (1964).

⁶B. Segall, *Phys. Rev.* **131**, 121 (1963). Dimensions around $(0.25, 0.25, 1)$ confirmed by Ashcroft's measurements [N. W. Ashcroft, *Phil. Mag.* **8**, 2055 (1963)]; cf. Ashcroft's Fig. 14 and Segall's Fig. 2(a) with the free-electron section inserted.

⁸W. A. Harrison, *Phys. Rev.* **116**, 557 (1959).

HIGH-ENERGY (0.1-2 MeV) FISSION CROSS-SECTION STRUCTURE MEASURED USING A NUCLEAR EXPLOSION IN SPACE*

Richard D. Albert

Lawrence Radiation Laboratory, University of California, Livermore, California

(Received 18 August 1965)

During the last U. S. high-altitude nuclear test series, an experiment to measure the fission cross sections of U^{233} and U^{235} was performed using a nuclear explosion as a source of neutrons.¹ The measurement was carried out above the earth's atmosphere over a neutron flight path of about 1300 km using sounding rockets to carry the fission and moderated BF_3 neutron detectors. A description of the experiment which includes gross cross-section data obtained over five decades of energy (30 eV to 5 MeV) has been previously presented.²

The purpose of this Letter is to report details of data obtained for the energy region above 100 keV where the fission cross section is characterized by large variations in amplitude as a function of incident neutron energy. The observed structure, which is shown in Fig. 1, has not been seen previously in laboratory data, which possess lower energy resolution.³ Our data, which were obtained with an experimental resolution of less than 1 nsec/m, are averaged over 10- to 30-keV energy intervals (indicated by the spacing between points) to reduce statistical errors and facilitate correlation analyses.

As seen in Fig. 1, structure appears in both

cross sections, although its features are more prominent in the U^{233} data, which exhibit variations of the order of three times the statistical error. (A solid curve has been drawn to delineate features that are believed to have statistical significance.)

An autocorrelation analysis of the U^{233} data

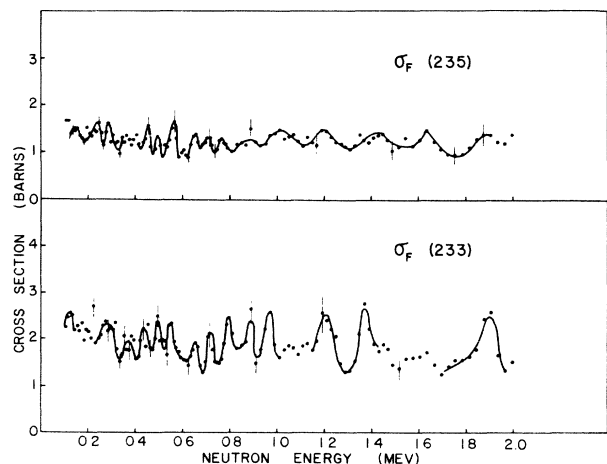


FIG. 1. U^{233} and U^{235} fission cross sections plotted against energy in the 0.1- to 2-MeV energy region.